CHARACTERIZATION OF HIGH ENTROPY ALLOYS $MnCrFe_2Ni_2$ AND $CoCrFe_2Ni_2$ WITH ADDITIONS IN DIFFERENT AMOUNTS OF Cu AND Mo AFTER HIGH TEMPERATURE THERMAL TREATMENTS

***César Fernández-Jiménez*[1], *Isaac Toda-Caraballo* [1], *Álvaro Ridruejo* [2], *David San-Martín* [1]**

[1]Materalia research group, Physical Metallurgy Department, CENIM-CSIC, Avda Gregorio del amo 8, 28040 Madrid, Spain; cesar.fernandez@cenim.csic.es
[2]Department of Materials Science, Polytechnic University of Madrid, E.T.S. de Ingenieros de Caminos, 28040 Madrid, Spain

Summary: Two high entropy alloy (HEAs) families, based on $CoCrFe_2Ni_2$ and $MnCrFe_2Ni_2$ compositions, with different additions of Cu and Mo, have been designed for high temperature applications. The $CoCrFe_2Ni_2$ alloys corresponds to the most studied system in the HEAs community, while in the $MnCrFe_2Ni_2$ alloys, Co is substituted by Mn in order to obtain more affordable alloys with similar or better mechanical properties and resistant to high temperatures in nuclear environments. The recrystallization and grain growth behaviour has been investigated in the initially deformed microstructure of these alloys between 1000 and 1200 °C (10 min holding time). Both alloy families fully recrystallize only after heating above 1100 °C. Segregation of Cu and Mn has been detected only at the grain boundaries of $MnCrFe_2Ni_2$ alloys, especially for the higher Cu contents and after heating above 1150 ºC. $MnCrFe_2Ni_2$ alloys possess a higher yield strength but a lower strain-hardening exponent.

Keywords: High entropy alloys, heat treatment, recrystallization, grain growth, segregation, chemical etching, SEM, EDS, mechanical characterization.

1. INTRODUCTION.

High entropy alloys (HEAs) [1-5] emerged in 2004 as a new paradigm in metallurgy. As opposite to classical metallurgy, where a principal element defines the alloy, HEAs are based on the use of several elements in similar content. The term was initial proposed by Yeh et al [5], although, independently, a work by Cantor et al [6] developed a similar concept which was defined as multi-principal element alloys (MPEAs) [6]. Both alloy concepts are closely related to each other and show a great number of possibilities in the development of new alloys.

The alloys that have been studied in this master's thesis are $CoCrFe_2Ni_2$ and $MnCrFe_2Ni_2$, both with additions in different amounts of Cu and Mo. A major limitation of the CoCrFeNi system is its mechanical properties [7], but on the other side, it has good microstructural stability [7-9]. Therefore, a large amount of research has been carried out investigating the influence of different additions of chemical elements, either to improve their mechanical properties or to improve other properties. The most relevant for this research work are solid solution hardening [10] and the exploration of TRIP/TWIP effects [11] without overly compromising their microstructural stability. On the other hand, a disadvantage of any alloy containing Co is that it cannot be applied in a nuclear radiation environment due to its activation. This is one reason why new HEAs are being developed to replace Co, which adds to its high price and scarce availability.

The use of Co is common in HEAs since it helps stabilizing the FCC phase. Once Co is removed, other FCC-stabilizer must be added. This is the case of Mn, which has been seen to help in the microstructural stability in HEAs, but also in commercial alloys, such as austenitic stainless steels, which make alloys based on the CrFeNiMn system attractive for nuclear applications [12,13].

Thus, in this project, the CoCrFeNi+Cu+Mo is studied, in parallel to the MnCrFeNi+Cu+Mo in order to investigate the Co-by-Mn replacement. The composition is selected according to the empirical solid solution formation rules, where Co (in the first family) is maintained with low content, as well as Cr in order to avoid σ-phase formation but high enough to keep oxidation resistance. Therefore, the compositions $CoCrFe_2Ni_2$ and $MnCrFe_2Ni_2$ are selected for the base alloys, and additions of Cu and Cu-Mo, in different amounts are included. The objective of this work is to study the recrystallization and grain growth behavior of these alloys after the application of different heat treatments between 1000 and 1200 ºC. Afterwards, mechanical properties of these microstructures were evaluated. The investigation is oriented to provide a deep insight into these alloys, and cover, at the same time, a wide range of microstructural and mechanical experimental skills.

2. METHODOLOGY.

In this master's thesis several compositional variations around two base alloys have been studied (Table 1**)**. The two base alloys have the designation A2 and MAT1 and have, as chemical composition, $CoCrFe_2Ni_2$ for A2 and

Table 1: High entropy alloys investigated in this research (as-designed). Compositions are provided in at.%.

		Co	Cr	Fe	Mn	Ni	Cu	Mo
$(CoCrFe_2Ni_2)_{0.9}(Cu_xMo_{1-x})_{0.1}$	A2_1	15	15	30	-	30	10	-
	A2_2	15	15	30	-	30	6.67	3.33
	A2_3	15	15	30	-	30	5	5
$(MnCrFe_2Ni_2)_{0.9}(Cu_xMo_{1-x})_{0.1}$	MAT1_1	-	15	30	15	30	10	-
	MAT1_2	-	15	30	15	30	6.67	3.33
	MAT1_3	-	15	30	15	30	5	5

$MnCrFe_2Ni_2$ for MAT1. The samples have been homogeneized at 1200 °C for 5 h and hot-forged just after being removed from the furnace, and air cooled to room temperature. After the process of homogenization and forging, the alloys were subjected to different heat treatments (Table 2) using the heating and cooling system of a dilatometer.

Table 2. Heat treatment conditions investigated. HR stands for Heating Rate, T is the temperature, t is the holding time and CR is the cooling rate.

	HR [°C/s]	T [°C]	t [s]	CR [°C/s]
A2_1, A2_3	5	1000, 1050, 1100, 1150,1200	600	50
A2_2, MAT1	5	1100, 1150, 1200	600	50

A detailed characterization of the samples was carried out using optical microscopy, SEM, XRD, hardness tests and compression tests. The heat treated samples were prepared using standard metallographic techniques, finishing with a 0.25 µm diamond cloth. The grain boundaries were revealed using either using electrolytic etching with oxalic acid (10 %) or Kalling's nº 2.

3. RESULTS AND DISCUSSION.

Firstly, to reveal the grain boundaries, several etchants have been tested. In this regard, kalling's 2 reagent has given the best results in MAT1 alloys, whereas electrolytic etching with an oxalic acid solution has worked better for the A2 alloys.

Figure 1 shows two examples of the microstructures obtained after the application of the homogeneization and hot forging treatments (alloys A2_1 and MAT1_1). Similar microstructures have been observed in all the alloys investigated. These optical images reveal that dynamic recrystallization has barely occurred during hot-forging; some recrystallized regions coexist with large areas that remain deformed, suggesting that the recrystallization temperatures (T_r) of A2 and MAT1 alloys is located at very high temperatures. Therefore, the deformed microstructures possess a high thermal stability, comparable to nickel-based superalloys [14-15]. X-ray diffraction analysis performed in all these microstructures confirm that A2 and MAT1 alloys possess an FCC single-phase crystal structure.

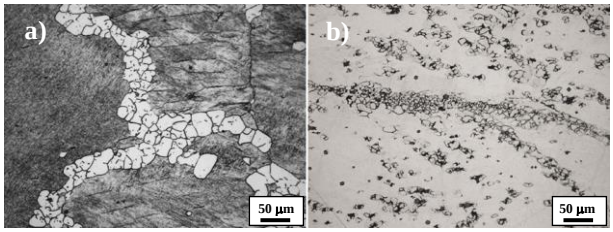

Figure 1. Light optical images of the microstructure of the alloys a) A2_1 and b) MAT1_1 after the homogeniezation at 1200 °C for 5 h and hot forging plus air-cooling to room temperature.

With the aim of recrystallizing the microstructure shown in Figure 1, the alloys have been subjected to the heat treatments described in Table 2. Surprisingly, the A2 alloys do not recrystallize after heating to 1000 °C and 1050 °C and holding for 10 minutes (images not shown), confirming the high thermal stability of these microstructures. Only after heating to or above 1100 °C, a complete recrystallization has been achieved within 10 minutes. It should be mentioned that longer holding times than those tested in this work should likely promote recrystallization at lower temperatures. However, the lower the temperature, the longer this time should be. Figure 2 provides several examples of recrystallized microstructures in some of the alloys investigated at 1100 and 1200 ºC.

The micrographs have been digitally treated to obtain a detailed description of the grain size distribution. Table 3 summarizes the average grain size (with the associated standard error) for all the alloys and conditions analysed. As it would be expected, the larger the heating temperature, the larger the grain size for a given alloy. Besides, A2 alloys have larger average grain sizes than MAT1 ones. In Figure 2, it can be also realized that in MAT1_1 alloy the grain boundaries appear severely etched in black at temperatures higher than 1100 ºC (see Figure 2f**)**. Similar behaviour has also been detected in the MAT1_2 alloy.

Along with the average grain size values, Table 3 summarizes the activation energies (Q) for grain growth. These have been estimated considering a parabolic grain growth law:

$$d^2-d^2_0=kt \quad (1)$$

With d the grain size and t the time, and an Arrhenius type of equation for parameter k:

$$k=k_0\exp(-Q/RT) \quad (2)$$

Table 3. Average grain size vs temperature and activation energy Q for the alloys.

	Grain Size [μm]			Q [KJ/mol]
	1100 °C	1150 °C	1200 °C	
A2_1	83.7 ± 3.6	126.5 ± 8.5	151.6 ± 10.4	374
A2_2	88.6 ± 5.2	118.3 ± 8.6	162.5 ± 8.1	358
A2_3	62.4 ± 2.3	115.0 ± 5.4	259.7 ± 18.4	369
MAT1_1	29.2 ± 0.8	37.6 ± 1.4	45.4 ± 1.3	405
MAT1_2	45.7 ± 2.1	60.5 ± 2.6	76.7 ± 5.0	391
MAT1_3	61.5 ± 3.9	86.0 ± 7.0	158.5 ± 11.3	370

With R the ideal gas constant and T the temperature. In MAT1 alloys, the higher the amount of Cu, the higher the activation energy, due to the co-segregation of Cu-Mn at the grain boundaries, which lowered their mobility and decelerated the grain growth.

To investigate further the etching response observed in MAT1 alloys, as-polished samples of the microstructures of alloy MAT1_1 obtained after heating to 1150 and 1200 ºC have been inspected using backscatter electron (BSE) images (Figure 3a and b, respectively). These images also show that a second lighter phase seems to be present at the grain boundaries. Energy dispersive spectroscopy (EDS) line scans (yellow dash lines) and point analysis S1-S2 (see results in Table 4) confirm the presence of Cu and Mn segregated at the grain boundary. This type of segregation during thermal treatments is a major problem in many Cu added alloys, since the presence of these Cu/Mn rich regions lowers the melting temperature at these locations [16]. In this regard, softening (bending) of the samples has been observed during heating, especially in alloy MAT1_1 after heating to 1200 ºC. This segregation behaviour has not been detected in A2 alloys.

Table 4. EDS point analyses pointed out by white arrows in Figure 3c (Alloy MAT1_1 - 1200 °C held for 10 min). The analysis are provided in at.%.

MAT1_1 1200 °C	O	Cr	Mn	Fe	Ni	Cu
S 1	-	3.3	20.1	7.1	18.1	51.4
S 2	-	3.7	20.0	7.5	20.6	48.2
S 3	-	15.8	10.7	32.6	29.3	11.6
S 4	-	15.6	11.2	30.4	30.7	12.1
S 5	62.6	25.4	12.0	-	-	-

To complement the microstructural characterization, compression tests have been carried out to investigate the mechanical behaviour of alloys A2 and MAT1. From these compression test, the yield strength has been determined. In addition, the strain hardening exponent (n) has been obtained after fitting the experimental stress-strain curve to Eq (3):

$$\sigma = C_0 \varepsilon^n \quad (3)$$

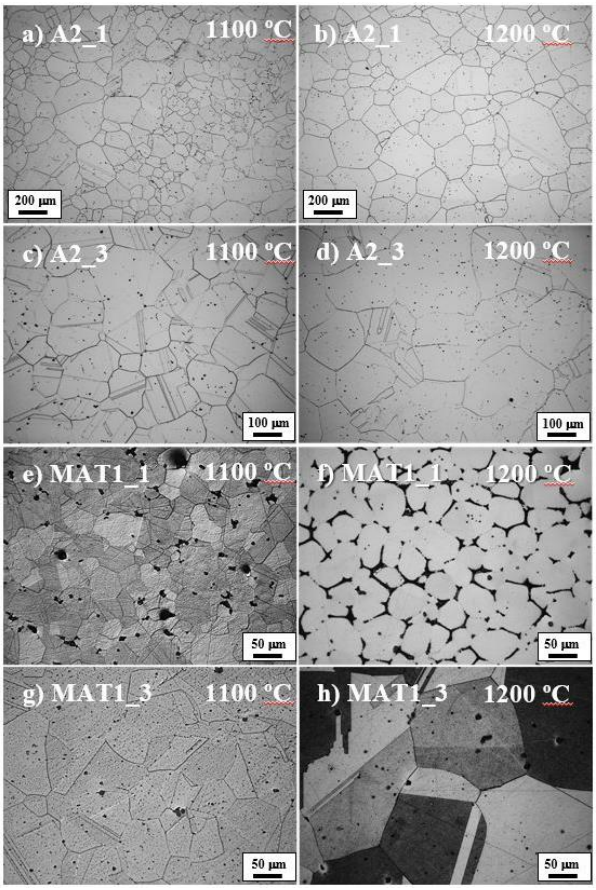

Figure 2. Light optical micrographs of the microstructure of alloys A2_1 (a,b); A2_3 (c,d); MAT1_1 (e,f) and MAT1_3 (g,h) after heating to 1100 and 1200 ºC and holding for 10 min. Images a) to d) have been taken under bright field illumination while e) to h) using Nomarski differential interference contrast (DIC) microscopy.

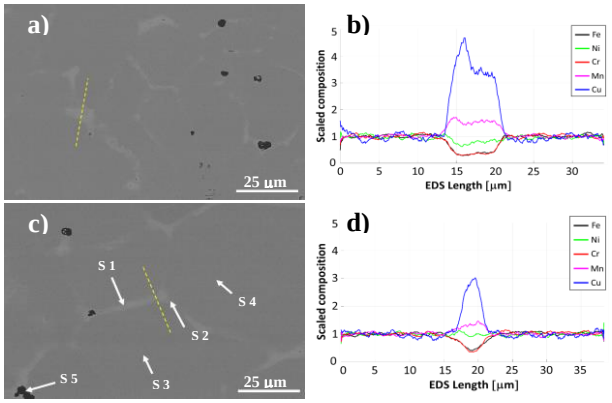

Figure 3. SEM-BSE images of the microstructure MAT1_1, after heating to a) 1150 and c) 1200 ºC. The yellow dashed line shows the location where the EDS line analysis have been measured (results shown in plots b) and d). Labels S1 – S5 show where the point EDS analyses have been performed in c). The results have been summarized in Table 4.

In this equation, σ is the true stress, ε the true strain, C_0 is the strength coefficient and n the strain hardening exponent. In the plot depicted in Figure 4, the strain hardening exponent is compared against the yield strength for the two alloy families (A2 and MAT1).

Two areas with different properties have been highlighted with an ellipse. The MAT1 alloys have a higher yield strength but a lower strain hardening exponent compared to A2 alloys. This is likely related to the presence of Mn, used as a substitute for Co in the composition of MAT1 alloys. The expected strengthening effect of Mo is more obvious in the MAT1 alloys. In addition, a different behaviour is observed when comparing each alloy heat treated at different temperatures; alloys treated at 1200 ºC (marked with ×) have a lower work hardening ability than the alloys treated at lower temperatures, where the best performance is observed in the samples heat treatments at 1100 ºC (marked with dots).

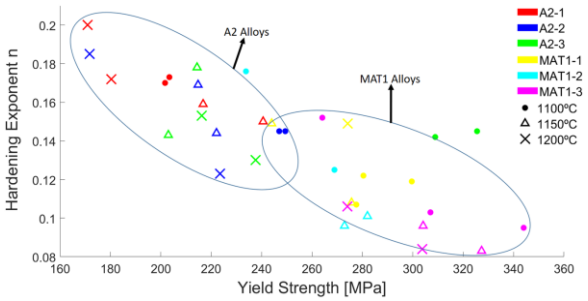

Figure 4. Strain hardening exponent vs yield strength.

4. CONCLUSIONS.

The following main conclusions can be highlighted from this investigation concerned with the influence of different heat treatments on the recrystallization and grain growth behaviour of two different families of high entropy alloys (A2 and MAT1) as well as their mechanical compression performance:

1) Kalling's 2 reagent has been demonstrated to reveal clearly the grain boundaries in MAT1 alloys, whereas an electrolytic solution of 10 % oxalic acid works best for A2 alloys.

2) Only after heating to 1100 ºC the initially deformed, hot-forged microstructure of both alloy families MAT1 and A2 can be recrystallized after 10 min holding time, pointing out the high recrystallization temperature (T_r). This result along with the high activation energy for grain growth estimated for these alloys show that they possess a high thermal stability.

3) High temperature heat treatments performed in alloys MAT1_1 and MAT1_2 at 1150 ºC and 1200 ºC promote the co-segregation of Cu and Mn at the grain boundaries, reaching values of ~50 at.% Cu, ~20 at.% Ni and Mn, and ~10 at.% of Fe+Cr. The decrease in Cu and increase in Mo, minimizes this segregation so that it was not detected in MAT1_3. In addition, the absence of this segregation in the Co-alloyed (A2) samples, suggest that the presence of Co avoids this segregation.

4) Compression tests performed in both alloy families show that MAT1 alloys have a higher yield strength and a lower strain hardening exponent than A2 alloys. This can be attributed to the presence of Mn, used as a substitute for Co in the composition of MAT1 alloys. The expected strengthening effect of Mo is only relevant in the MAT1 alloys and not so evident in A2 alloys.

5. REFERENCES.

[1] Chen T.K., Shun T.T., Yeh J.-W., Wong M.S., Nanostructured nitride films of multi-element high-entropy alloys by reactive DC sputtering, Surf. Coat. Technol. 188-189 (2004) 193-200.

[2] Hsu C.-Y., Yeh J.-W., Chen S.-K., Shun T.-T., Wear resistance and high temperature compression strength of FCC CuCoNiCrAl0.5Fe alloy with boron addition, Metall. Mater. Trans. A 35 (2004) 1465-1469.

[3] Huang P.-K., Yeh J.-W., Shun T.-T., Chen S.-K., Multi-principal-element alloys with improved oxidation and wear resistance for thermal spray coating, Adv Eng. Mater. 6 (2004) 74-78.

[4] Yeh J.-W., Chen S.-K., Gan J.-W., Lin S.-J., Chin T.-S., Shun T.-T., Tsau C.-H., Chang S.- Y., Formation of simple crystal structures in Cu-Co-Ni-Cr-Al-Fe-Ti-V alloys with multiprincipal metallic elements, Metall. Mater. Trans. A 35 (2004) 2533-2536.

[5] Yeh J.-W., Chen S.-K., Lin S.-J., Gan J.-Y., Chin T.-S., Shun T.-T., Tsau C.-H., Chang S.-Y., Nanostructured high-entropy alloys with multiple principal elements: Novel alloy design concepts and outcomes, Adv. Eng. Mater. 6 (2004) 299-303.

[6] Cantor B., Chang I.T.H., Knight P., Vincent A.J.B., Microstructural development in equiatomic multicomponent alloys, Mater. Sci. Eng. A 375-377 (2004) 213-218.

[7] Zaddach A. J., Scattergood R. O., and Koch C. C., "Tensile properties of low-stacking fault energy high-entropy alloys," Mater. Sci. Eng. A 636 (2015) 373-378.

[8] Wang W. R., Wang W. L., and Yeh J. W., "Phases, microstructure and mechanical properties of AlxCoCrFeNi high-entropy alloys at elevated temperatures," J. Alloys Compd., 589, (2014), 143-152.

[9] Brif Y., Thomas M., and Todd I., "The use of high-entropy alloys in additive manufacturing," Scr. Mater. 99 (2015) 93-96.

[10] Isaac Toda-Caraballo, Pedro E.J. Rivera-Díaz-del-Castillo, Modelling solid solution hardening in high entropy alloys, Acta Mater. 85 (2015) 14-23.

[11] Li Z., Tasan C. C., Springer H., Gault B., and Raabe D., "Interstitial atoms enable joint twinning and transformation induced plasticity in strong and ductile high-entropy alloys," Sci. Rep., 7 (2017) 1-7.

[12] Wu Z., Bei H., Microstructures and mechanical properties of compositionally complex Co-free FeNiMnCr18 FCC solid solution alloy, Mater. Sci. Eng. A 640 (2015) 217-224.

[13] Kumar N., Li C., Leonard K., Bei H., Zinkle S., Microstructural stability and mechanical behavior of FeNiMnCr high entropy alloy under ion irradiation, Acta Mater. 113 (2016) 230-244,

[14] Humphreys F.J., Hatherly M., Recrystallization and related annealing phenomena, Kidlington, Oxford OX5 1GB, UK, Elsevier Ltd, (2004)

[15] Wang Y., Shao W.Z., Zhen L., Zhang X.M., Microstructure evolution during dynamic recrystallization of hot deformed superalloy 718, Mater. Sci. Eng. A 486 (2008) 321-332.

[16] Roya R.K., Panda A.K., Das S.K., Govind, Mitra A., "Development of a copper-based filler alloy for brazing stainless steels", Mater. Sci. Eng. A 523 (2009) 312-315.